Article

Journal of Vibration and Control
2015, Vol. 21(9) 1667–1679

DOI: 10.1177/1077546313500061
jvc.sagepub.com

Improving the ride comfort of vehicle passenger using fuzzy sliding mode controller

Yunus Ziya Arslan, Aziz Sezgin and Nurkan Yagiz

Abstract

Attenuation of the adverse effects of vehicle vibrations on human health is a challenging problem. One common approach to solve this problem is to use various types of controllers in vehicle suspensions. In this study, in order to decrease the vehicle vibrations and hence improve the ride comfort, a fuzzy logic integrated sliding mode controller was designed. The performance of the controller was tested in a biodynamic human-vehicle combined model. The human body was considered as a lumped parameter model and incorporated into a full vehicle model. The biodynamic responses of a human body to vehicle vibrations were analyzed. Performances of the conventional sliding mode and fuzzy integrated sliding mode controllers were compared with those of a passive control strategy. According to the numerical results, the fuzzy sliding mode controller overcame both classic sliding mode and passive control approaches and decreased vehicle vibrations considerably. It can be deduced from the study that active suspension systems would play a key role in decreasing the negative effects of vehicle vibrations on human health, such as motion sickness, discomfort and spine injuries.

Keywords

Full vehicle model, fuzzy sliding mode control, human biodynamic model, ISO 2631, whole body vibration

1. Introduction

Limitation of physiological and psychological effects of vehicle vibrations on passengers is still a challenging problem and attenuation of vehicle vibrations using active control methods is an active research area in control engineering (Guclu, 2003; Wang et al., 2006; Jianmin and Qingmei, 2007; Yagiz and Hacioglu, 2008; Huang et al., 2010). The biodynamic response of a human body to vibration is the key indicator for evaluation of passenger ride comfort (Griffin and Paddan, 2002; Papalukopoulos and Natsiavas, 2007). Vibration transmitted from a seat to the human body is absorbed by the tissue and organs, and this situation results in some symptoms within the human body, such as motion sickness, discomfort, loss of performance, back injuries and even spine fracture (Rasmussen, 1983; Seidel, 1993).

One common approach to minimize vehicle vibration and limit the adverse effects of vibration on human health is to employ the various controllers in suspension systems (Kuo and Hseng, 1999; Guclu, 2005; Choi and Han, 2007; Sezgin and Arslan, 2012). Sliding mode is one of the widely used controllers in vehicle suspension systems (Kim and Ro, 1998; Yagiz et al., 2000; Yoshimura et al., 2001). A sliding mode controller (SMC) guarantees the system's stability, i.e. it shows a robust behavior and it has a relatively simple structure (Utkin, 1977). Yuksek et al. (2002) used a chattering-free sliding mode controller in suspension systems of a full vehicle model and they reported that this controller method was successfully applicable to nonlinear systems with superior performance.

Department of Mechanical Engineering, Faculty of Engineering, Istanbul University, Turkey

Received: 4 September 2012; accepted: 2 July 2013

Corresponding author:
Aziz Sezgin, İstanbul Üniversitesi Mühendislik Fakültesi Makina Mühendisliği Bölümü, 34320 Avcılar, İstanbul, Turkey.
Email: asezgin@istanbul.edu.tr

In recent years, several studies have been undertaken to combine the merits of classical sliding mode control and intelligent techniques such as fuzzy logic and neural networks. Ertugrul and Kaynak (2000) reported that the main idea behind this notion is the elimination of the requirement on exact knowledge of plant dynamics and on the smoothing of the control input. Fuzzy logic is one of the most preferred methods that are combined with sliding mode control to tune the system parameters. Nowadays, there are many application areas of fuzzy sliding mode controller (FSMC), such as robotics (Arslan et al., 2009), vehicle suspension (Yagiz et al., 2008) and braking systems (Lin and Hsu, 2003), seismic isolation of earthquake-excited structures (Alli and Yakut, 2005) and so on. Yagiz et al. (2008) integrated a non-chattering sliding mode controller with fuzzy unit and applied this controller to a four-degrees-of-freedom (d.f.) half vehicle model. In their proposed controller, the fuzzy logic algorithm continuously updated the slope constant of the sliding surfaces of the sliding-mode controller according to the controlled states of the system. They reported that by using the proposed controller algorithm, the magnitudes of the body displacement and pitch motion were decreased, and resonance peak due to the vehicle body was eliminated.

In this study, to improve the ride comfort of a vehicle occupant subjected to whole body vibration, fuzzy integrated sliding mode controller was designed and tested in a human-vehicle model. Numerical results obtained from the fuzzy sliding mode controller were compared with those obtained from both the conventional sliding mode controller and the passive control approach. The biodynamic response of the human body to vehicle vibrations was also discussed.

2. Modeling

In the literature, lumped parameter models of the human body are considered as several concentrated masses interconnected by springs and dampers (Liang and Chiang, 2006). Since these models are simple to analyze and relatively easy to validate with experiments, they are commonly used in the human body modeling studies (Muksian and Nash, 1974; Boileau and Rakheja, 1998). Liang and Chiang (2006) conducted a study on lumped-parameter human body models for seated human subjects without backrest support under vertical vibration excitation. They analyzed and validated the models by the synthesis of various experimental data from published literature. They reported in their extensive review study that based on the analytical study and experimental validation, the four-d.f. model developed by Wan and Schimmels (1995) was best fitted to the existing test results. They recommended this model for the prospective studies of biodynamic responses of seated human subjects under vertical body vibration. Therefore, in this study, to receive the biodynamic response of the human body to vehicle vibrations, the human body model proposed by Wan and Schimmels (1995) was used. This biodynamic human model was incorporated into a seven-d.f. full vehicle model (Figure 1).

The human body was segmented into four parts in the model. The body was formed with four separate masses interconnected by five sets of springs and dampers, with a total human mass of 60.67 kg (Liang and Chiang, 2006). A seat was also added to the model which transmits the vertical vehicle vibrations to the human body. Biomechanical values of human body parts, namely masses (m_7, m_8, m_9, m_{10}), springs (k_7, k_{79}, k_8, k_9, k_{10}) and dampers (b_7, b_{79}, b_8, b_9, b_{10}), along with the spring and damping coefficients of the seat (k_6, b_6), are given in Appendix A.

The vehicle model has seven d.f., which are due to body bounce y_5, roll α, pitch θ and vertical motion of each wheel y_i ($i = 1, 2, 3, 4$). In the model, unsprung masses (wheel-axle assembly), sprung mass (vehicle body), and mass moment of inertia for the roll and pitch motions of the vehicle body were denoted by m_i, m_5, I_α and I_θ, respectively. Coefficients of the linear damping and linear springs are b_i, k_i, k_{5i}, respectively and y_{0i} are the road inputs to wheels. Distances of the suspensions to the center of mass of the vehicle body were denoted by l_1, l_2, l_3, l_4 and distances between the center of gravity and the passenger seat by s_x, s_z. Velocity of the vehicle in x-direction is represented by V. In addition, u_i represents the control force applied to suspensions. By taking the seat into account, the total d.f. of the human-vehicle model becomes 12. Numerical values of the vehicle parameters are given in Appendix A. Equations of motion of the human-vehicle model in state space form can be given as follows:

$$\dot{\mathbf{x}} = \mathbf{f}(\mathbf{x}) + \mathbf{B}\underline{\mathbf{u}} \tag{1}$$

where $\mathbf{x} = [x_1\ x_2\ x_3 \ldots x_{24}]^T$ is state vector and equals to $\left[y_5\ \theta\ \alpha\ y_1\ y_2\ y_3\ y_4\ y_6 \ldots y_{10}\ \dot{y}_5\ \dot{\theta}\ \dot{\alpha}\ \dot{y}_1\ \dot{y}_2\ \dot{y}_3\ \dot{y}_4\ \dot{y}_6\ \ldots\ \dot{y}_{10}\right]^T$. $\mathbf{f}(\mathbf{x})$ is the vector of the state equations without control inputs, $\mathbf{B}$ is the control force matrix and $\underline{\mathbf{u}} = \left[u_1\quad u_2\quad u_3\quad u_4\right]$ is the vector of the control forces applied to the system.

In the study, it was assumed that the vehicle vibrations only stemmed from the unevenness of the road surface. Sayers (1995) proposed a well accepted indicator of longitudinal unevenness level called the International Roughness Index, which gives information about the quality of road profiles. In this index,

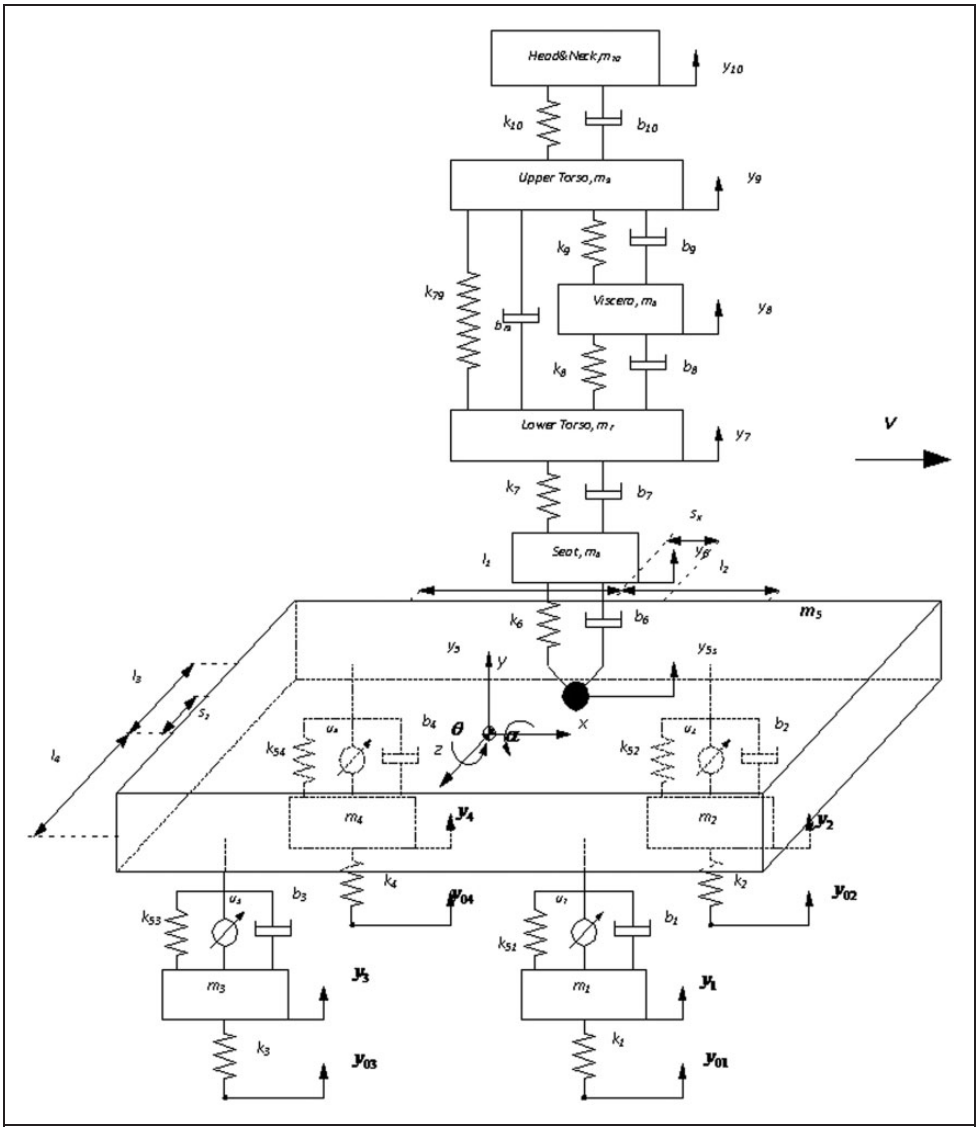

Figure 1. The combined human-vehicle model.

road profiles are created by combining the random and harmonic vibrations. The road elevation used in this study can be expressed as follows:

$$H(l) = (1 - q)\, H_0(l) + q\, H_1(l) \tag{2}$$

where $H_0(l)$ and $H_1(l)$ are the random and harmonic components of the road profile depending on the distance l along the track, respectively and q is a proportion of the random and harmonic components contribution to the road profile. Since the vehicle was assumed to travel with a constant velocity of 20 m/s for 5 seconds, the road roughness was considered as a disturbance to the model for a distance of 100 m (Figure 2). Further details representing the calculation of the road roughness and the road parameters are given in Appendix C.

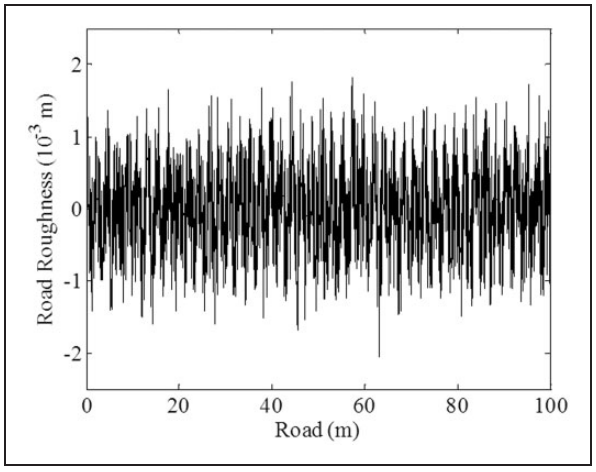

Figure 2. Road roughness applied to the model as disturbance.

3. The controller design

Following the pioneering study of Utkin (1977), the sliding mode control approach encouraged many investigators to apply this method for the suppression of the undesired vibrations (Kim and Ro, 1998; Yagiz et al., 2000; Yoshimura et al., 2001). One of the major advantages of this controller method is its robust behavior, namely it is insensitive to parameter variations and external disturbances. Yagiz (2004) demonstrated that implementation of the SMC in vehicle suspension systems considerably improved the ride comfort. In this study, to improve the performance of the classical sliding mode approach, fuzzy tuning was incorporated in this control system.

3.1. Sliding mode controller design

The sliding mode controller used in this study was designed according to the principles defined by Utkin (1993). The sliding surface was selected as

$$\boldsymbol{\sigma} = \mathbf{G}\,\Delta\mathbf{x} \tag{3}$$

where $\Delta\mathbf{x}$ is the difference between the reference value $\mathbf{x_r}$ and the corresponding state $\mathbf{x}$. $\mathbf{G}$ stands for the positive sliding slopes.

$$\mathbf{G} = \begin{bmatrix} \alpha_1 & 0 & 0 & 0 & 0 & 1 & 0 & 0 & 0 & 0 \\ 0 & \ddots & 0 & 0 & 0 & 0 & \ddots & 0 & 0 & 0 \\ 0 & 0 & \alpha_i & 0 & 0 & 0 & 0 & 1 & 0 & 0 \\ 0 & 0 & 0 & \ddots & 0 & 0 & 0 & 0 & \ddots & 0 \\ 0 & 0 & 0 & 0 & \alpha_n & 0 & 0 & 0 & 0 & 1 \end{bmatrix}_{n\,x2n} \tag{4}$$

For stability analysis, Lyapunov function candidate was selected such that it is positive definite and its derivative is negative semi-definite.

$$\mathbf{v}(\boldsymbol{\sigma}) = \frac{\boldsymbol{\sigma}^{\mathrm{T}}\boldsymbol{\sigma}}{2} > 0 \tag{5}$$

$$\frac{\mathrm{d}\mathbf{v}(\boldsymbol{\sigma})}{\mathrm{d}t} = \frac{\dot{\boldsymbol{\sigma}}^{\mathrm{T}}\boldsymbol{\sigma}}{2} + \frac{\boldsymbol{\sigma}^{\mathrm{T}}\dot{\boldsymbol{\sigma}}}{2} \le 0 \tag{6}$$

If $\Delta\mathbf{x} = \mathbf{x_r} - \mathbf{x}$ is incorporated into equation (3) then

$$\boldsymbol{\sigma} = \mathbf{G}\,\mathbf{x_r} - \mathbf{G}\,\mathbf{x} \tag{7}$$

is obtained. Equation (7) can be reformed as

$$\boldsymbol{\sigma} = \boldsymbol{\Phi}(t) - \boldsymbol{\sigma}_{\mathbf{a}}(\mathbf{x}) \tag{8}$$

where $\boldsymbol{\Phi}(t) = \mathbf{G}\,\mathbf{x_r}$ and $\boldsymbol{\sigma}_{\mathbf{a}}(\mathbf{x}) = \mathbf{G}\,\mathbf{x}$.

Derivation of equation (8) is

$$\frac{\mathrm{d}\boldsymbol{\sigma}}{\mathrm{d}t} = \frac{\mathrm{d}\boldsymbol{\Phi}(t)}{\mathrm{d}t} - \frac{\delta\boldsymbol{\sigma}_{\mathbf{a}}(\mathbf{x})}{\delta x}\frac{\mathrm{d}\mathbf{x}}{\mathrm{d}t} \tag{9}$$

If the limit case of the controller is applied to equation (6) and from equation (1) and (3)

$$\frac{\mathrm{d}\boldsymbol{\Phi}(t)}{\mathrm{d}t} - \mathbf{G}\left(\mathbf{f}(\mathbf{x}) + \mathbf{B}\,\mathbf{u}_{eq}\right) = 0 \tag{10}$$

Then the controller force for the limit case is obtained as

$$\mathbf{u}_{\mathrm{eq}} = (\mathbf{GB})^{-1}\left(\frac{\mathrm{d}\boldsymbol{\Phi}(t)}{\mathrm{d}t} - \mathbf{G}\,\mathbf{f}(\mathbf{x})\right) \tag{11}$$

As the controller force for the limit case is only valid on the sliding surface, an additional term should be defined to pull the system to the surface. For this purpose, derivative of the Lyapunov function can be selected as

$$\dot{\mathbf{v}}(\boldsymbol{\sigma}) = -\sigma^{\mathrm{T}}\boldsymbol{\Gamma}\boldsymbol{\sigma} < 0 \tag{12}$$

where $\boldsymbol{\Gamma}$ is positive definite matrix and its values are decided by means of a trial and error method until satisfactory results are obtained.

$$\boldsymbol{\Gamma} = \begin{bmatrix} \Gamma_1 & 0 & 0 & 0 & 0 \\ 0 & \ddots & 0 & 0 & 0 \\ 0 & 0 & \Gamma_i & 0 & 0 \\ 0 & 0 & 0 & \ddots & 0 \\ 0 & 0 & 0 & 0 & \Gamma_n \end{bmatrix}_{nxn} \tag{13}$$

By using equation (6), along with equations (9) and (12)

$$\boldsymbol{\sigma}^{\mathrm{T}}\dot{\boldsymbol{\sigma}} = -\boldsymbol{\sigma}^{\mathrm{T}}\boldsymbol{\Gamma}\sigma \Rightarrow \frac{\mathrm{d}\boldsymbol{\sigma}}{\mathrm{d}t} + \boldsymbol{\Gamma}\sigma = 0 \tag{14}$$

$$\frac{\mathrm{d}\boldsymbol{\sigma}}{\mathrm{d}t} + \boldsymbol{\Gamma}\sigma = \frac{\mathrm{d}\boldsymbol{\Phi}(t)}{\mathrm{d}t} - \mathbf{G}(\mathbf{f}(\mathbf{x}) + \mathbf{B}\,\mathbf{u}) + \boldsymbol{\Gamma}\,\boldsymbol{\sigma} = 0 \tag{15}$$

$$\mathbf{u} = (\mathbf{GB})^{-1}\left(\frac{\mathrm{d}\boldsymbol{\Phi}(t)}{\mathrm{d}t} - \mathbf{G}\,\mathbf{f}(\mathbf{x})\right) + (\mathbf{GB})^{-1}\boldsymbol{\Gamma}\,\boldsymbol{\sigma} \tag{16}$$

Using equation (11), total control input can be written as

$$\mathbf{u} = \mathbf{u}_{\mathrm{eq}} + (\mathbf{GB})^{-1}\,\boldsymbol{\Gamma}\sigma \tag{17}$$

Here $(\mathbf{GB})^{-1}$ always equals to mass matrix. But $\mathbf{f}(\mathbf{x})$ and $\mathbf{B}$ are not well-known. Thus, in this study equivalent control was calculated using the average of the

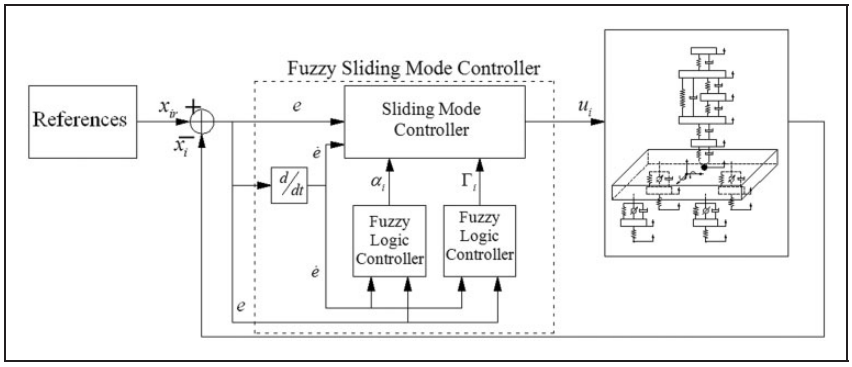

Figure 3. Block diagram of the fuzzy sliding mode controlled human-vehicle model.

total control. For this purpose a low-pass filter was used. This filter was designed as

$$\tau\dot{\hat{\mathbf{u}}}_{\mathrm{eq}} + \hat{\mathbf{u}}_{\mathrm{eq}} = \mathbf{u} \tag{18}$$

where τ is the time constant of the low pass filter. Finally, the control input can be written as

$$\mathbf{u} = \hat{\mathbf{u}}_{\mathrm{eq}} + (\mathbf{GB})^{-1}\,\boldsymbol{\Gamma}\sigma \tag{19}$$

3.2. Fuzzy sliding mode controller design

Many parameters of the controllers that play key roles in attenuation of the vibrations are determined according to the designers' experiences, i.e. by trial and error method. However, since this approach is subjective, it is not a convenient method to find the best parameters to suppress the unwanted vibrations of the investigated system. Fuzzy logic is one of the preferred approaches to determine the controller parameters (Visioli, 2001). This approach may be able to avoid possible shortcomings stemming from the designer's subjective decisions. For this purpose, SMC was tuned by a fuzzy logic algorithm in this study. The sliding surface slopes α_i and elements of the positive definite matrix $\boldsymbol{\Gamma}$ were determined using fuzzy logic. Using this approach, different values were assigned to α_i and $\boldsymbol{\Gamma}$ for each iteration cycle. The diagram in Figure 3 denotes this loop in which the fuzzy logic algorithm tunes the parameters of SMC for each cycle.

The membership functions and their limits for the error, the derivative of error, α_i and Γ_i are presented in Figure 4. The constructed fuzzy associative memory (FAM) table that shows the fuzzy control rules can be seen in Table 1. Abbreviations used in the table are as follows:

VVS: very very small, VS: very small, S: small, M: medium, B: big, VB: very big, VVB: very very big, NB: negative big, NM: negative medium, NS: negative small, Z: zero, PS: positive small, PM: positive medium, PB: positive big.

A representative rule that can be extracted from the FAM table is:

$$\text{If } e : NB \text{ and } \dot{e} : NB \text{ THEN } \alpha_i : M \text{ and } \Gamma_i : M (i = 1, 2, 3)$$

4. Numerical results and discussion

Long-term exposure to whole body vibration especially at low frequencies may cause permanent health disorders in the internal organs, muscles and bone structure. Rasmussen (1983) reported some symptoms and the corresponding frequency levels as follows: influence on breathing movements at 4–8 Hz, general feeling of discomfort and muscle contractions at 4–9 Hz, abdominal pains at 4–10 Hz, chest pains at 5–7 Hz, lower jaw symptoms at 6–8 Hz, urge to urinate at 10–18 Hz, head symptoms, influence on speech and increased muscle tone at 13–20 Hz. In addition to these health problems, the vibration with strong acceleration may cause serious spinal column disease and other spinal complaints (Hulshof and Zanten, 1987).

The physiological response of the human body to the vibration exposure mainly depends on the amplitude, duration and frequency of vibration. Displacement-time histories of the human body parts modeled in this study are shown in Figure 5. By comparing the magnitudes of the vertical vibrations for active and passive (uncontrolled) suspensions it can be observed that the active suspension systems considerably reduce the vibration amplitude and hence improve the ride comfort (Figure 5).

As the force generated by the inertia is related to body acceleration, the vertical acceleration of the human body parts is also an important criterion that gives insight into the ride comfort of a seat's occupant,

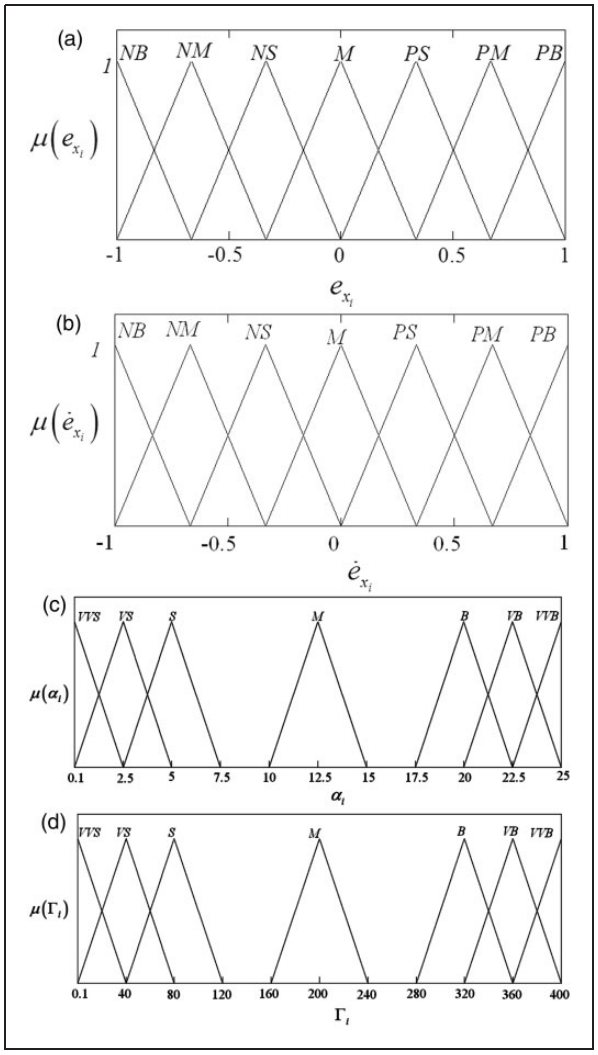

Figure 4. Membership functions of the fuzzy sliding mode controller for: (a) error; (b) derivation of the error; (c) sliding surface slopes, α_i and (d) elements of .

Table 1. FAM table.

		Derivative of error						
		NB	*NM*	*NS*	*Z*	*PS*	*PM*	*PB*
Error	*NB*	M	B	VB	VVB	VB	B	M
	NM	S	M	B	VB	B	M	S
	NS	VS	S	M	B	M	S	VS
	Z	VVS	VS	S	M	S	VS	VVS
	PS	VS	S	M	B	M	S	VS
	PM	S	M	B	VB	B	M	S
	PB	M	B	VB	VVB	VB	B	M

along with the vertical displacement (Yuksek et al., 2002). In this study, assessment of the mechanical vibration effects on the human body were performed according to International Standard ISO 2631 (1997). In ISO 2631 (1997), in addition to the mechanical responses, physiological effects due to vehicle vibrations are also evaluated (Rasmussen, 1983). Although the limits of the human body to vibration exposure were given as recommendations rather than firm boundaries in ISO 2631, in many studies these criteria are considered as quantitative physiological limits for healthy people (Griffin, 1998; Bovenzi and Hulshof, 1999; Abercromby et al., 2007). For a prolonged vibration exposure, the standard provides human vibration sensitivity curves for health effects, such as lumbar spinal disorders and motion sickness. These curves were specified by taking into account the magnitude and frequency of acceleration and the duration of exposure to the acceleration.

Comparison of the root mean square (RMS) accelerations of the human body parts obtained from different cases, i.e., uncontrolled, sliding mode controlled and fuzzy sliding mode controlled cases with the criteria defined in ISO 2631 (1997), are presented in Figure 6. The peaks in the acceleration RMS graphs indicate that the corresponding frequency of excitation coincides with the natural frequency of the system. It can be clearly seen from Figure 6 that FSMC reduced the magnitudes of RMS acceleration of human body parts more than the passive case and SMC.

In the uncontrolled case, it can be seen from the results that the passenger exposed to ride vibrations felt head and neck, upper torso and viscera symptoms for up to four hours; and lower torso symptoms for between four and six hours. In controlled cases, magnitudes of the vibrations on the human body parts are considerably less than those of the uncontrolled case. Unlike in the uncontrolled case, possible symptoms that may occur in the sliding mode controlled case are seen after a travel duration of six hours. In the fuzzy sliding mode controlled case, ride duration without adverse effects of vibration was increased such that symptoms appeared after the travel duration of nearly 12 hours.

The natural frequencies of the sprung and unsprung masses were estimated as 1.2 Hz and 9.5 Hz for the vehicle, respectively. It can be deduced from Figure 6 that unsprung masses lead the system to have a peak around the frequency of 9 Hz. Moreover, another peak can be seen in the fuzzy sliding controlled case around the frequency of 7 Hz. This peak level is also seen under the different road profiles. Since the natural frequency of the seat was found as 6.7 Hz, this peak could be related to the mass of the vehicle seat.

The road holding (Figure 7) and suspension deflection (Figure 8) were also taken into account. The suspension system must support the vehicle, provide directional control and isolation of passengers from vibrations which are directly related to suspension

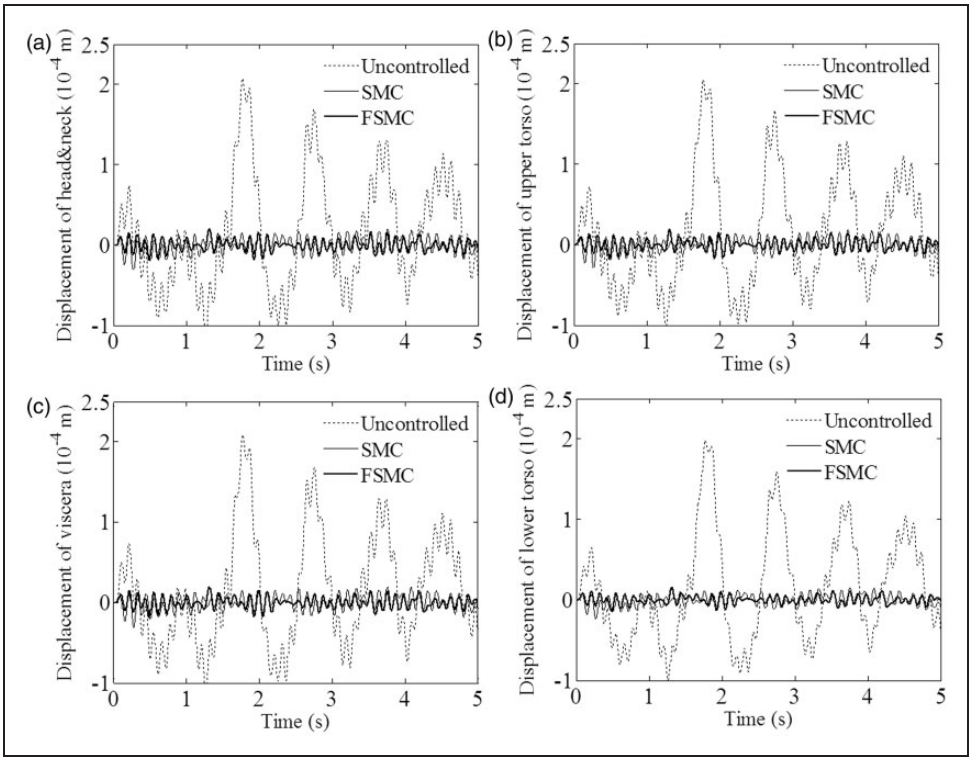

Figure 5. Time responses of the human body parts.

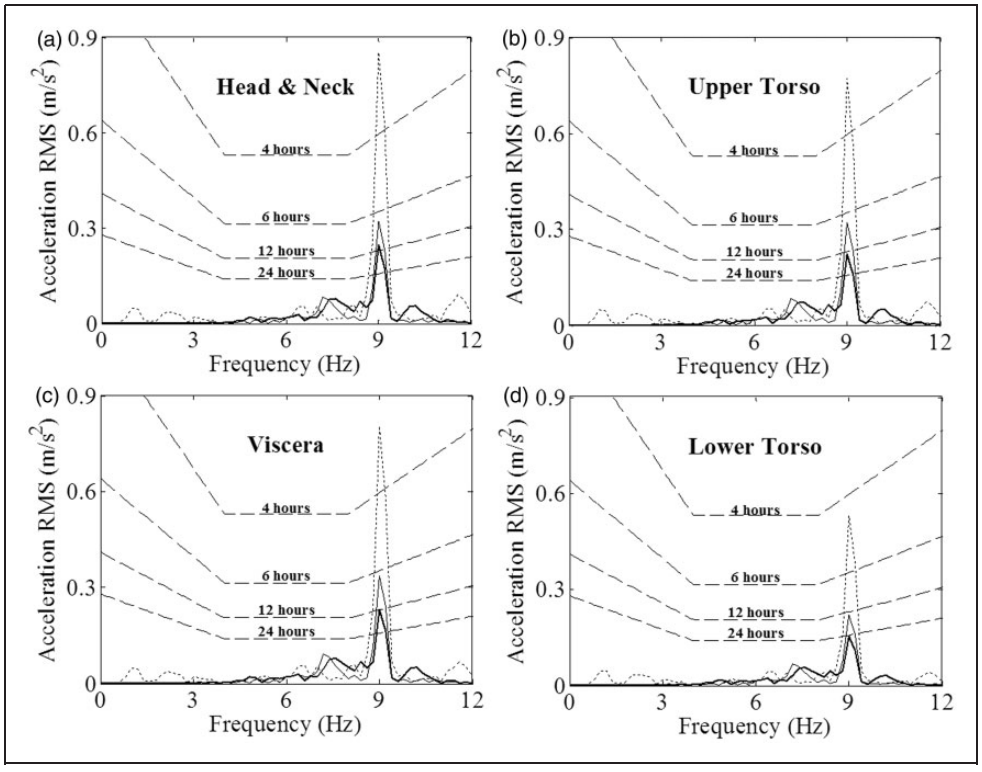

Figure 6. Comparison of root mean square (RMS) accelerations of (a) head and neckl; (b) upper Torso and (c) viscera; (d) lower torso obtained in uncontrolled (dotted line), sliding mode controlled (solid line) and fuzzy sliding mode controlled cases (bold solid line). Dashed lines indicate the human vibration sensitivity curves associated with duration of vibration exposure, frequency and acceleration.

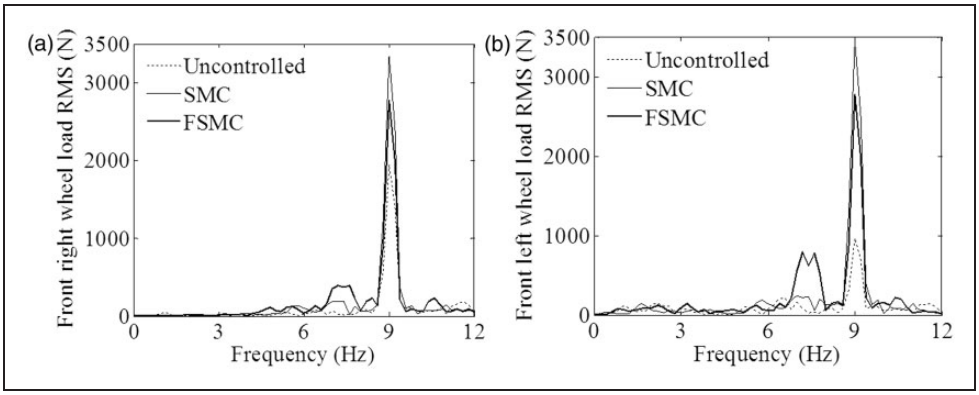

Figure 7. Dynamic wheel loads for (a) front right; (b) front left.

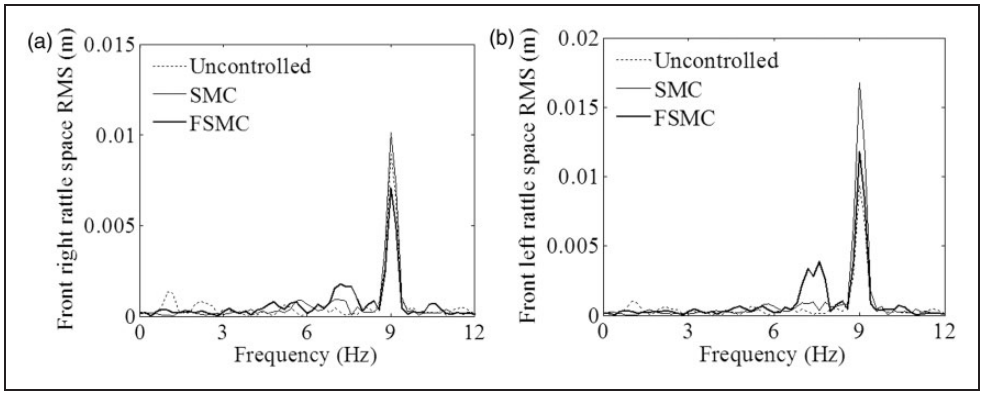

Figure 8. Suspension deflections for (a) front right; (b) front left.

deflection, road holding and ride comfort, respectively (Wright and Williams, 1984). However, it is a fact that there is a trade-off between ride comfort and road holding for passive suspension systems (Collette and Preumont, 2010). Hence improving the ride comfort of a vehicle may affect the road holding and suspension deflection.

To investigate the ride safety, i.e. the road holding performance of the vehicle, dynamic wheel loads can be used as indicators. Dynamic wheel loads for front wheels over a frequency range are given in Figure 7. It can be observed from the figure that for active suspensions, dynamic wheel loads get higher, improving the road holding performance.

In order to observe whether the relative deflection of the suspension exceeds the mechanical limits, rattle spaces of the vehicle were investigated. Suspension deflections of the vehicle were given in Figure 8. It can be observed from the figures that maximum magnitude of the suspension deflection is nearly 0.018 m and the magnitude of the rattle space stays in acceptable limits.

In order to investigate the three dimensional movements of the vehicle, pitch and roll motions of the vehicle body are given in Figure 9. Success of both controllers in suppressing the vibrations can be observed from these figures.

The controller forces of the system can be seen in Figure 10. There is another trade-off between ride comfort and controller forces; the better the ride comfort, the higher the controller forces. For the front suspension systems, FSMC and SMC require similar control forces in magnitude; they have the maximum controller force of 175 N, which is a reasonable value for a linear force actuator.

To give insight into how the values of α_i and Γ_i changed in the fuzzy integrated control application, variation of α_1 and Γ_1 are given in Figure 11. It can be seen from the figure that fuzzy algorithm tuned α_1 and Γ_1 nearly between 0.1 and 30 and between 40 and 150, respectively.

The main advantages of fuzzy logic controllers are representing the knowledge relatively easily in the form of linguistic rules and encompassing a great complexity with few rules. Once the fuzzy logic part is designed, there is no difficulty in using fuzzy logic with SMC. The strategy in adjusting the sliding slope is unique and once constructed in fuzzy logic, it is independent of

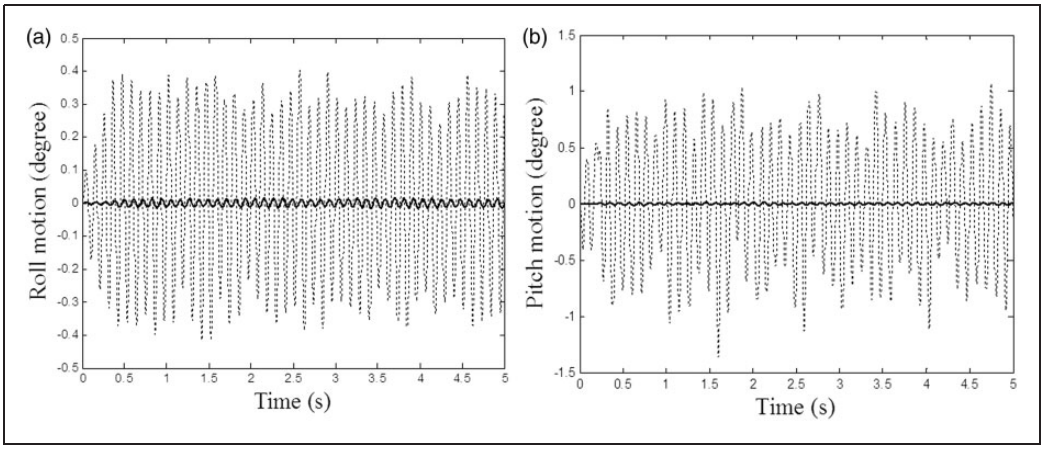

Figure 9. Variation of (a) roll motion and (b) pitch motion of the vehicle for the uncontrolled (dotted line), sliding mode controlled (solid line) and fuzzy sliding mode controlled cases (bold solid line).

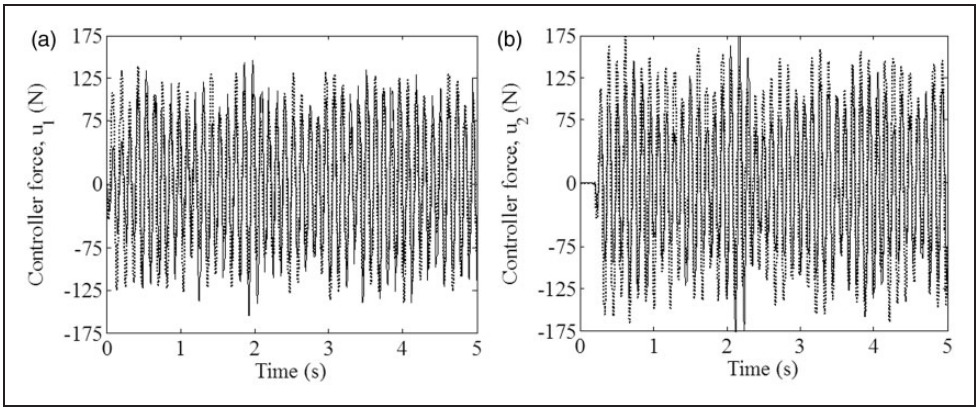

Figure 10. Controller forces for (a) front right and (b) front left obtained in sliding mode (dotted line) and fuzzy sliding mode controlled cases (solid line).

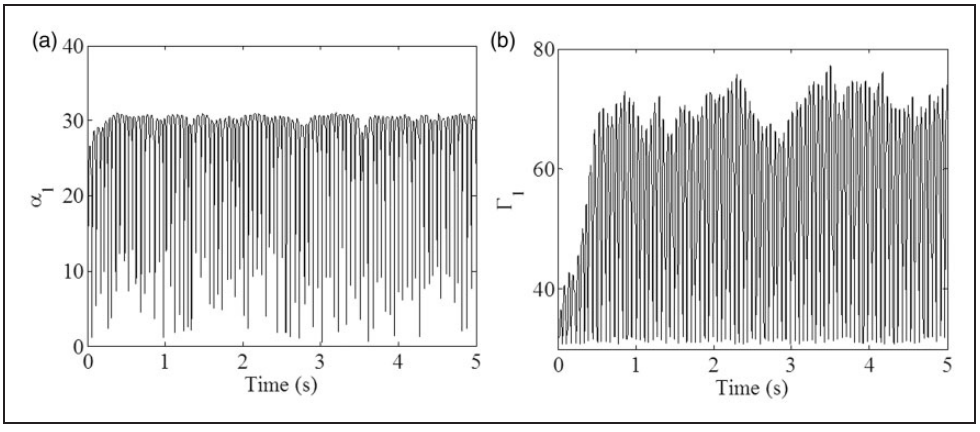

Figure 11. Variation of (a) α_1 and (b) Γ_1.

the system. On the other hand SMC partly ensures stability because it depends on the Lyapunov stability criterion (Ha et al., 2001). However, FSMC has some limitations in determining suitable membership functions and fuzzy rules. The performance of the controller depends mainly on the experience of the control designer. Therefore, it faces some challenges in fine-tuning and hence requires more simulations before being applied to a system (Yagiz et al., 2008).

5. Conclusions

In this study, in order to improve the ride comfort of vehicles, classical and fuzzy tuned sliding mode controllers were designed. These controllers were applied to a human-vehicle model and their performances were compared with that of the passive suspension system. Displacement and acceleration responses of the human body segments demonstrated that fuzzy integrated and classical sliding mode controllers improved ride comfort considerably more than the passive controller. Moreover, the fuzzy sliding mode controller overcame the classical sliding mode approach in suppressing the vibrations. It can be concluded from the obtained results that active suspension systems, especially artificial intelligence integrated systems, may improve the ride comfort and decrease the health risks of vibrations for vehicle occupants.

Acknowledgements

The authors would like to thank Dr. Yuksel Hacioglu for his thoughtful reading and valuable remarks.

Funding

This research received no specific grant from any funding agency in the public, commercial, or not-for-profit sectors.

References

Abercromby AFJ, Amonette WE, Layne CS, McFarlin BK, Hinman MR and Paloski WH (2007) Vibration exposure and biodynamic responses during whole-body vibration training. *Medicine and Science in Sports and Exercise* 39(10): 1794–1800.

Alli H and Yakut O (2005) Fuzzy sliding-mode control of structures. *Engineering Structures* 27(2): 277–284.

Arslan YZ, Hacioglu Y and Yagiz N (2009) Fuzzy sliding mode control of a finger of a humanoid robot hand. *Expert Systems* 26(3): 291–303.

Boileau PE and Rakheja S (1998) Whole-body vertical biodynamic response characteristics of the seated vehicle passenger: measurement and model development. *International Journal of Industrial Ergonomics* 22: 449–472.

Bovenzi M and Hulshof CTJ (1999) An updated review of epidemiologic studies on the relationship between exposure to whole-body vibration and low back pain (1986–1997). *International Archives of Occupational and Environmental Health* 72: 351–365.

Choi SB and Han YM (2007) Vibration control of electrorheological seat suspension with human-body model using sliding mode control. *Journal of Sound and Vibration* 303: 391–404.

Collette C and Preumont A (2010) High frequency energy transfer in semi-active suspension. *Journal of Sound and Vibration* 329: 4604–4616.

Ertugrul M and Kaynak O (2000) Neuro sliding mode control of robotic manipulators. *Mechatronics* 10(1–2): 239–263.

Griffin MJ (1998) A comparison of standardized methods for predicting the hazards of whole-body vibration and repeated shocks. *Journal of Sound and Vibration* 215: 883–914.

Griffin MJ and Paddan GS (2002) Effect of seating on exposures to whole-body vibration in vehicles. *Journal of Sound and Vibration* 253(1): 215–241.

Guclu R (2003) Active control of seat vibrations of a vehicle model using various suspension alternatives. *Turkish Journal of Engineering and Environmental Science* 27: 361–373.

Guclu R (2005) Fuzzy logic control of seat vibrations of a non-linear full vehicle model. *Nonlinear Dynamics* 40: 21–34.

Ha QP, Nguyen QH, Rye DC and Durrant-Whyte HF (2001) Fuzzy sliding mode controllers with applications. *IEEE Transactions of Industrial Electronics* 48(1): 38–46.

Huang CJ, Lin JS and Chen CC (2010) Road-adaptive algorithm design of half-car active suspension system. *Expert Systems with Applications* 37: 4392–4402.

Hulshof C and Zanten BV (1987) Whole-body vibration and low-back pain. *International Archives of Occupational and Environmental Health* 59(3): 205–220.

ISO 2631-1*Mechanical Vibration and Shock – Evaluation of Human Exposure to Whole – Body VibrationPart 1: General Requirements*.

Jianmin S and Qingmei S (2007) On vibration control methods of vehicle. In *Proceedings of the 26th Chinese Control Conference,* July 2007, Hunan, China, pp. 71–74.

Kim C and Ro PI (1998) A sliding mode controller for vehicle active suspension systems with non-linearities. In *Proceedings of the Institution of Mechanical Engineers, Part D: Journal of Automobile* 212(2): 79–92.

Kuo YP and Hseng TLS (1999) GA-based fuzzy PI/PD controller for automotive active suspension system. *IEEE Transactions on Industrial Electronics* 46(6): 1051–1056.

Liang CC and Chiang CF (2006) A study on biodynamic models of seated human subjects exposed to vertical vibration. *International Journal of Industrial Ergonomics* 36: 869–890.

Lin CM and Hsu CF (2003) Self-learning fuzzy sliding-mode control for antilock braking systems. *IEEE Transactions on Control Systems Technology* 11(2): 273–278.

Muksian R and Nash CD (1974) A model for the response of seated humans to sinusoidal displacements of the seat. *Journal of Biomechanics* 7: 209–215.

Papalukopoulos C and Natsiavas S (2007) Nonlinear biodynamics of passengers coupled with quarter car models. *Journal of Sound and Vibration* 304: 50–71.

Rasmussen G (1983) Human body vibration exposure and its measurement. *Journal of the Acoustical Society of America* 73(6): 2229–2229.

Sayers MW (1995) On the calculation of international roughness index from longitudinal road profile. *Transportation Research Record* 1501: 1–12.

Seidel H (1993) Selected health risks caused by long-term, whole-body vibration. *American Journal of Industrial Medicine* 23(4): 589–604.

Sezgin A and Arslan YZ (2012) Analysis of the vertical vibration effects on ride comfort of vehicle driver. *Journal of Vibroengineering* 14(2): 559–571.

Utkin VI (1977) Variable structure systems with sliding modes. *IEEE Transactions on Automatic Control* 22(2): 212–222.

Utkin VI (1993) Sliding mode control design principles and applications to electric drives. *IEEE Transactions on Industrial Electronics* 40(1): 23–36.

Visioli A (2001) Tuning of PID controllers with fuzzy logic. *IEE Proceedings – Control Theory and Applications* 148(1): 1–8.

Wan Y and Schimmels JM (1995) A simple model that captures the essential dynamics of a seated human exposed to whole body vibration. *Advances in Bioengineering, ASME* 31: 333–334.

Wang W, Rakheja S and Boileau PE (2006) The role of seat geometry and posture on the mechanical energy absorption characteristics of seated occupants under vertical vibration. *International Journal of Industrial Ergonomics* 36: 171–184.

Wright PG and Williams DA (1984) The application of active suspension to high performance road vehicles. In *Proceedings of the IMechE Conference on Microprocessors in Fluid Engineering*, Bath University, England, September 1984, pp. 23–38.

Yagiz N, Yuksek I and Sivrioglu S (2000) Robust control of active suspensions for a full vehicle model using sliding mode control. *JSME International Journal, Series C* 43(2): 253–258.

Yagiz N (2004) Comparison and evaluation of different control strategies on a full vehicle model with passenger seat using sliding modes. *International Journal of Vehicle Design* 34(2): 168–182.

Yagiz N and Hacioglu Y (2008) Backstepping control of a vehicle with active suspensions. *Control Engineering Practice* 16(12): 1457–1467.

Yagiz N, Hacioglu Y and Taskin Y (2008) Fuzzy sliding-mode control of active suspensions. *IEEE Transactions on Industrial Electronics* 55(11): 3883–3890.

Yoshimura T, Kume A, Kurimoto M and Hino J (2001) Construction of an active suspension system of a quarter car model using the concept of sliding mode control. *Journal of Sound and Vibration* 239(2): 187–199.

Yuksek I, Yagiz N, Kikushuma Y and Tanaka N (2002) Sliding mode control of a full vehicle with non-linearity. In: *The 6th International Conference on Motion and Vibration Control,* 19–23 August 2002*,* Saitama, Japan.

Appendix A

Table 2. Numerical values of the parameters used in the study.

m_1	: 66.50 kg	b_3	: 935 Ns/m	k_{51}	: 27000 N/m	l_1	: 1.945 m
m_2	: 66.50 kg	b_4	: 935 Ns/m	k_{52}	: 27000 N/m	l_2	: 2.115 m
m_3	: 45.18 kg	b_6	: 500 Ns/m	k_{53}	: 20770 N/m	l_3	: 0.58 m
m_4	: 45.18 kg	b_7	: 2475 Ns/m	k_{54}	: 20770 N/m	l_4	: 1.16 m
m_5	: 1380 kg	b_{79}	: 909.1 Ns/m	k_6	: 500.0 N/m	V	: 20 m/s
m_6	: 28.00 kg	b_8	: 330 Ns/m	k_7	: 49,350 N/m	q	: 0.1
m_7	: 36.00 kg	b_9	: 200 Ns/m	k_{79}	: 192,000 N/m	Γ_1	: 75
m_8	: 5.50 kg	b_{10}	: 250 Ns/m	k_8	: 20,000 N/m	Γ_2	: 75
m_9	: 15.00 kg	k_1	: 211180 N/m	k_9	: 10,000 N/m	Γ_3	: 75
m_{10}	: 4.17 kg	k_2	: 211180 N/m	k_{10}	: 134,400 N/m	α_1	: 1
b_1	: 2015 Ns/m	k_3	: 211180 N/m	s_z	: 0.785 m	α_2	: 1
b_2	: 2015 N/m	k_4	: 211180 N/m	s_x	: 0.295 m	α_3	: 1

Appendix B

Equations of motion of the human-vehicle model

$$\begin{aligned}
&I\ddot{\alpha} - k_{51}\cdot c\cdot \cos\alpha(y_5 + a\cdot \sin\theta - c\cdot \sin\alpha - y_1) + k_{52}\cdot d\cdot \cos\alpha(y_5 + a\cdot \sin\theta + d\cdot \sin\alpha - y_2)\\
&\quad - k_{53}\cdot c\cdot \cos\alpha(y_5 - b\cdot \sin\theta - c\cdot \sin\alpha - y_3) + k_{54}\cdot d\cdot \cos\alpha(y_5 - b\cdot \sin\theta + d\cdot \sin\alpha - y_4)\\
&\quad - k_6\cdot d\cdot \cos\alpha(y_6 - y_5 - a\cdot \sin\theta - d\cdot \sin\alpha) - b_1\cdot c\cdot \cos\alpha\left(\dot{y}_5 + a\cdot\dot{\theta}\cdot \cos\theta - c\cdot\dot{\alpha}\cdot \cos\alpha - \dot{y}_1\right)\\
&\quad + b_2\cdot d\cdot \cos\alpha\left(\dot{y}_5 + a\cdot\dot{\theta}\cdot \cos\theta + d\cdot\dot{\alpha}\cdot \cos\alpha - \dot{y}_2\right) - b_3\cdot c\cdot \cos\alpha\left(\dot{y}_5 - b\cdot\dot{\theta}\cdot \cos\theta - c\cdot\dot{\alpha}\cdot \cos\alpha - \dot{y}_3\right)\\
&\quad + b_4\cdot d\cdot \cos\alpha\left(\dot{y}_5 - b\cdot\dot{\theta}\cdot \cos\theta + d\cdot\dot{\alpha}\cdot \cos\alpha - \dot{y}_4\right) - b_6\cdot d\cdot \cos\alpha\left(\dot{x}_6 - \dot{x}_5 - a\cdot\dot{\theta}\cdot \cos\theta - d\cdot\dot{\alpha}\cdot \cos\alpha\right)\\
&= -cu_1 + du_2 - cu_3 + du_4
\end{aligned} \tag{B.1}$$

$$\begin{aligned}
&I\ddot{\theta} + k_{51}\cdot a\cdot \cos\theta(y_5 + a\cdot \sin\theta - c\cdot \sin\alpha - y_1) + k_{52}\cdot a\cdot \cos\theta(y_5 + a\cdot \sin\theta + d\cdot \sin\alpha - y_2)\\
&\quad + k_{53}\cdot b\cdot \cos\theta(y_5 - b\cdot \sin\theta - c\cdot \sin\alpha - y_3) - k_{54}\cdot b\cdot \cos\theta(y_5 - b\cdot \sin\theta + d\cdot \sin\alpha - y_4)\\
&\quad + k_6\cdot a\cdot \cos\theta(y_6 - y_5 - a\cdot \sin\theta - d\cdot \sin\alpha) + b_1\cdot a\cdot \cos\theta\left(\dot{y}_5 + a\cdot\dot{\theta}\cdot \cos\theta - c\cdot\dot{\alpha}\cdot \cos\alpha - \dot{y}_1\right)\\
&\quad + b_2\cdot a\cdot \cos\theta\left(\dot{y}_5 + a\cdot\dot{\theta}\cdot \cos\theta + d\cdot\dot{\alpha}\cdot \cos\alpha - \dot{y}_2\right) - b_3\cdot b\cdot \cos\theta\left(\dot{y}_5 - b\cdot\dot{\theta}\cdot \cos\theta - c\cdot\dot{\alpha}\cdot \cos\alpha - \dot{y}_3\right)\\
&\quad - b_4\cdot b\cdot \cos\theta\left(\dot{y}_5 - b\cdot\dot{\theta}\cdot \cos\theta + d\cdot\dot{\alpha}\cdot \cos\alpha - \dot{y}_4\right) - b_6\cdot a\cdot \cos\theta\left(\dot{y}_6 - \dot{y}_5 - a\cdot\dot{\theta}\cdot \cos\theta - d\cdot\dot{\alpha}\cdot \cos\alpha\right)\\
&= au_1 + au_2 - bu_3 - bu_4
\end{aligned} \tag{B.2}$$

$$\begin{aligned}
&m_5\cdot \ddot{y}_5 + k_{51}(y_5 + a\cdot \sin\theta - c\cdot \sin\alpha - y_1) + k_{52}(y_5 + a\cdot \sin\theta + d\cdot \sin\alpha - y_2)\\
&\quad + k_{53}(y_5 - b\cdot \sin\theta - c\cdot \sin\alpha - y_3) + k_{54}(y_5 - b\cdot \sin\theta + d\cdot \sin\alpha - y_4)\\
&\quad + b_1\left(\dot{y}_5 + a\cdot\dot{\theta}\cdot \cos\theta - c\cdot\dot{\alpha}\cdot \cos\alpha - \dot{y}_1\right) - k_6(y_6 - a\cdot \sin\theta - y_5 - d\cdot \sin\alpha)\\
&\quad + b_2\left(\dot{y}_5 + a\cdot\dot{\theta}\cdot \cos\theta + d\cdot\dot{\alpha}\cdot \cos\alpha - \dot{y}_2\right) + b_3\left(\dot{y}_5 - b\cdot\dot{\theta}\cdot \cos\theta - c\cdot\dot{\alpha}\cdot \cos\alpha - \dot{y}_3\right)\\
&\quad + b_4\left(\dot{y}_5 - b\cdot\dot{\theta}\cdot \cos\theta + d\cdot\dot{\alpha}\cdot \cos\alpha - \dot{y}_4\right) - b_6\left(\dot{y}_6 - a\cdot\dot{\theta}\cdot \cos\theta - \dot{y}_5 - d\cdot\dot{\alpha}\cdot \cos\alpha\right)\\
&= u_1 + u_2 + u_3 + u_4
\end{aligned} \tag{B.3}$$

$$\begin{aligned}
&m_1\cdot \ddot{y}_1 + k_1(y_1 - y_{01}) - k_{51}(y_5 + a\cdot \sin\theta - c\cdot \sin\alpha - y_1)\\
&\quad - b_1\left(\dot{y}_5 + a\cdot\dot{\theta}\cdot \cos\theta - c\cdot\dot{\alpha}\cdot \cos\alpha - \dot{y}_1\right) = -u_1
\end{aligned} \tag{B.4}$$

$$\begin{aligned}
&m_2\cdot \ddot{y}_2 + k_2(y_2 - y_{02}) - k_{52}(y_5 + a\cdot \sin\theta + d\cdot \sin\alpha - y_2)\\
&\quad - b_2\left(\dot{y}_5 + a\cdot\dot{\theta}\cdot \cos\theta + d\cdot\dot{\alpha}\cdot \cos\alpha - \dot{y}_2\right) = -u_2
\end{aligned} \tag{B.5}$$

$$\begin{aligned}
&m_3\cdot \ddot{y}_3 + k_3(y_3 - y_{03}) - k_{53}(y_5 - b\cdot \sin\theta - c\cdot \sin\alpha - y_3)\\
&\quad - b_3\left(\dot{y}_5 - b\cdot\dot{\theta}\cdot \cos\theta - c\cdot\dot{\alpha}\cdot \cos\alpha - \dot{y}_3\right) = -u_3
\end{aligned} \tag{B.6}$$

$$\begin{aligned}
&m_4\cdot \ddot{y}_4 + k_4(y_4 - y_{04}) - k_{54}(y_5 - b\cdot \sin\theta + d\cdot \sin\alpha - y_4)\\
&\quad - b_4\left(\dot{y}_5 - b\cdot\dot{\theta}\cdot \cos\theta + d\cdot\dot{\alpha}\cdot \cos\alpha - \dot{y}_4\right) = -u_4
\end{aligned} \tag{B.7}$$

$$m_6\cdot \ddot{y}_6 + k_6(y_6 - y_5 - a\cdot \sin\theta - d\cdot \sin\alpha) - k_7(y_7 - y_6) + b_6\left(\dot{y}_6 - \dot{y}_5 - a\cdot\dot{\theta}\cdot \cos\theta - d\cdot\dot{\alpha}\cdot \cos\alpha\right) = 0 \tag{B.8}$$

$$m_7\cdot \ddot{y}_7 + k_7(y_7 - y_6) - k_8(y_8 - y_7) - k_{79}(y_9 - y_7) + b_7(\dot{y}_7 - \dot{y}_6) - b_8(\dot{y}_8 - \dot{y}_7) - b_{79}(\dot{y}_9 - \dot{y}_7) = 0 \tag{B.9}$$

$$m_8\cdot \ddot{y}_8 + k_8(y_8 - y_7) - k_9(y_9 - y_8) + b_8(\dot{y}_8 - \dot{y}_7) - b_9(\dot{y}_9 - \dot{y}_8) = 0 \tag{B.10}$$

$$m_9\cdot \ddot{y}_9 + k_9(y_9 - y_8) - k_{10}(y_{10} - y_9) + k_{79}(y_9 - y_7) + b_9(\dot{y}_9 - \dot{y}_8) - b_{10}(\dot{y}_{10} - \dot{y}_9) + b_{79}(\dot{y}_9 - \dot{y}_7) = 0 \tag{B.11}$$

$$m_{10}\cdot \ddot{y}_{10} + k_{10}(y_{10} - y_9) + b_{10}(\dot{y}_{10} - \dot{y}_9) = 0 \tag{B.12}$$

Control force matrix [**B**]

$$[\mathbf{B}] = \begin{bmatrix} 0 & 0 & 0 & 0 \\ 0 & 0 & 0 & 0 \\ 0 & 0 & 0 & 0 \\ 0 & 0 & 0 & 0 \\ 0 & 0 & 0 & 0 \\ 0 & 0 & 0 & 0 \\ 0 & 0 & 0 & 0 \\ 0 & 0 & 0 & 0 \\ 0 & 0 & 0 & 0 \\ 0 & 0 & 0 & 0 \\ 0 & 0 & 0 & 0 \\ 0 & 0 & 0 & 0 \\ 1/m_5 & 1/m_5 & 1/m_5 & 1/m_5 \\ a/I_\theta & a/I_\theta & -b/I_\theta & -b/I_\theta \\ -c/I_\alpha & d/I_\alpha & -c/I_\alpha & d/I_\alpha \\ -1/m_1 & 0 & 0 & 0 \\ 0 & -1/m_2 & 0 & 0 \\ 0 & 0 & -1/m_3 & 0 \\ 0 & 0 & 0 & -1/m_4 \\ 0 & 0 & 0 & 0 \\ 0 & 0 & 0 & 0 \\ 0 & 0 & 0 & 0 \\ 0 & 0 & 0 & 0 \\ 0 & 0 & 0 & 0 \end{bmatrix} \tag{B.13}$$

Appendix C

Road roughness.

$$H_1(l) = A_d \cdot \cos(2\pi l/l_1) \tag{C.1}$$

where A_d is the amplitude of the harmonic undulation, and l_1 is its wavelength.

$$A_d = \sqrt{2D_0 q/(1-q)} \tag{C.2}$$

where, D_0 is the partial variances of the $H_0(l)$ and was expressed as follows

$$D_0 = C(2\pi)^{-w+1}(w-1)^{-1}\left(L_M^{w-1} - L_m^{w-1}\right) \tag{C.3}$$

In the equation, C is the unevenness index and w is the waviness. The value of w usually ranges from 1.5 to 3, with the typical value $w = 2$. L_M and L_m are the wavelength range of effectively acting wavelengths of the random road unevenness.